Published in final edited form as:
Cancer Res. 2014 December 15; 74(24): 7371–7382. doi:10.1158/0008-5472.CAN-14-0794.

Mig-6 suppresses endometrial cancer associated with *Pten* deficiency and ERK activation

Tae Hoon Kim[1,†], **Jung-Yoon Yoo**[1,8,†], **Hong Im Kim**[1], **Jenifer Gilbert**[2], **Bon Jeong Ku**[3], **Jane Li**[4], **Gordon B. Mills**[4], **Russell R. Broaddus**[5], **John P. Lydon**[6], **Jeong Mook Lim**[7], **Ho-Geun Yoon**[8,*], and **Jae-Wook Jeong**[1,*]

[1]Department of Obstetrics, Gynecology & Reproductive Biology, Michigan State University College of Human Medicine, Grand Rapids, MI 49503, USA [2]Institute of Immunology, National University of Ireland, Maynooth, Ireland [3]Department of Internal Medicine, Chungnam National University School of Medicine, Daejeon, 301-721, South Korea [4]Department of Systems Biology, The University of Texas M.D. Anderson Cancer Center, Houston, TX 77030, USA [5]Department of Pathology, The University of Texas M.D. Anderson Cancer Center, Houston, TX 77030, USA [6]Department of Molecular and Cellular Biology, Baylor College of Medicine, Houston, TX 77030, USA [7]Department of Agricultural Biotechnology, Seoul National University, Seoul 151-742, South Korea [8]Department of Biochemistry and Molecular Biology, Brain Korea 21 PLUS Project for Medicine Science, Yonsei University College of Medicine, Seoul 120-752, South Korea

Abstract

PTEN mutations are the most common genetic alterations in endometrial cancer. Loss of PTEN and subsequent AKT activation stimulate ERα-dependent pathways that play an important role in endometrial tumorigenesis. The major pathologic phenomenon of endometrial cancer is the loss of ovarian steroid hormone control over uterine epithelial cell proliferation and apoptosis. However, the precise mechanism of PTEN/AKT signaling in endometrial cancer remains poorly understood. The progesterone signaling mediator MIG-6 suppresses estrogen signaling and it has been implicated previously as a tumor suppressor in endometrial cancer. In this study, we show that MIG-6 also acts as a tumor suppressor in endometrial cancers associated with PTEN deficiency. Transgenic mice where *Mig-6* was overexpressed in PR-expressing cells exhibited a relative reduction in uterine tumorigenesis caused by *Pten* deficiency. ERK1/2 was phosphorylated in uterine tumors and administration of an ERK1/2 inhibitor suppressed cancer progression in $PR^{cre/+}Pten^{f/f}$ mice. In clinical specimens of endometrial cancer, MIG-6 expression correlated inversely with ERK1/2 phosphorylation during progression. Taken together, our findings suggest that *Mig-6* regulates ERK1/2 phosphorylation and that it is crucial for progression of PTEN-

[*]Correspondence to: Jae-Wook Jeong, Ph.D., Department of Obstetrics, Gynecology & Reproductive Biology, Michigan State University College of Human Medicine, 333 Bostwick Avenue NE, Suite 4024, Grand Rapids, MI 49503, Phone: 616-234-0987, Fax: 616-234-0990, JaeWook.Jeong@hc.msu.edu. Ho-Geun Yoon, Ph.D., Department of Biochemistry and Molecular Biology, Severance Medical Research Institute, Yonsei University College of Medicine,134 Shinchon-dong, Seodaemoon-gu, 120-752, Seoul, South Korea, Tel: +82-2-2228-1683, Fax: +82-2-312-5041, yhgeun@yuhs.ac.
[†]T.H.K. and J.Y.Y. contributed equally to this work.

The authors disclose no potential conflicts of interest.

mutant endometrial cancers, providing a mechanistic rationale for the evaluation of ERK1/2 inhibitors as a therapeutic treatment in human endometrial cancer.

Introduction

Endometrial cancer is the most common gynecological cancer (1). In the United States, approximately 47,130 cases will be diagnosed and 8,190 women die from the disease in 2013 (2). Endometriod carcinoma comprises 70–80% of cases and originate in epithelial cells of the endometrium (1). An increased incidence of endometrial cancer has been found in association with prolonged, unopposed estrogen exposure (3) and aberrant activation of the PTEN/PI3K/AKT and ErbB/ERK signaling pathways (1). *PTEN* is one of the most frequently mutated tumor suppressor genes in human cancers (4). PTEN is completely lost or mutated in >50% of primary endometrioid endometrial cancers and in at least 20% of endometrial hyperplasias (5). PTEN acts as a negative regulator of PI3K signaling, which regulates a number of cellular functions through the activation of AKT (6). Loss of PTEN resulted in the activation of ERα-dependent pathways that play an important role in the tumorigenesis of endometrial cancer (7). The PTEN/PI3K/AKT signaling pathway can also be activated by estrogen and growth factor, suggesting a cross-talk between PTEN/PI3K/AKT and ErbB/ERK signaling pathways (8). However, the relationship between PTEN/PI3K/AKT and ErbB/ERK signaling pathways has remained elusive.

Progesterone antagonizes the growth-promoting properties of estrogen in the uterus (9). Progesterone therapy prevents the development of endometrial cancer associated with unopposed estrogen by blocking estrogen actions (10). Progestin has been used in the conservative endocrine treatment to early endometrial cancer patients in order to preserve their fertility, as well as in palliative treatment to advanced-stage patients (11). Expression of progesterone receptor (PR) was known as positively correlated with a good prognosis and response to progestin treatment (12). However, objective responses were detected in 30% to as many as 56% of patients with metastatic or recurrent endometrial carcinoma (13). Therefore, the effectiveness of progestin for women with endometrial cancer is less clear.

Mitogen inducible gene 6 (*Mig-6*, *Errfi1*, *RALT*, or *gene 33*) is an immediate early response gene that can be induced by various mitogens and commonly occurring chronic stress stimuli (14). Ablation of *Mig-6* in mice leads to the development of animals with epithelial hyperplasia, adenoma, and adenocarcinomas in organs (15, 16). Decreased expression of *Mig-6* is observed in human breast carcinomas which correlate with reduced overall survival of breast cancer patients (17). Previously, we demonstrated that *Mig-6* is an important mediator of progesterone signaling to suppress estrogen signaling in the uterus (16). Ablation of *Mig-6* in the murine uterus leads to the development of endometrial hyperplasia and estrogen-induced endometrial cancer (16, 18). MIG-6 plays a tumor suppressor function in the context of *Pten* ablation (19). However, the mechanism by which *Mig-6* alters endometrial cancer pathophysiology remains unknown.

In this study, we utilized conditional overexpression of *Mig-6* in the $PR^{cre/+}Pten^{f/f}$ ($Pten^{d/d}$) mice to demonstrate that *Mig-6* is an important tumor suppressor in *Pten* deficient cancer. $PR^{cre/+}Mig\text{-}6^{over}Pten^{f/f}$ ($Mig\text{-}6^{over}Pten^{d/d}$) mice suppressed to develop endometrial cancer

through inhibition of ERK1/2 phosphorylation. The correlation studies showed an inverse correlation between MIG-6 and phospho-ERK1/2 in human endometrial cancer. Thus, these results demonstrate that *Mig-6* mediates progesterone action to suppress development and progression of endometrial cancer by inhibiting ERK1/2 signaling.

Materials and Methods

Construction of the targeting vectors and generation of *Mig-6^{Over}* mice

The targeting vector contains *Mig-6* cDNA, two ROSA26 genomic sequences for gene targeting (5′- and 3′-arms), a CMV early enhancer/chicken beta actin (CAG) promoter, and a loxP-STOP-loxP (LSL) cassette. The linearized targeting construct was transfected into R1 ES cells by electroporation (Figure S1A). Puromycin-resistant clones were screened by Southern blot analysis using 5′ external probes with EcoRV digested genomic DNA (Figure S1B). Correctly targeted clones were microinjected into blastocysts derived from C57BL/6 mice. Chimeras were bred to C57BL/6 mice and F1 agouti offspring mice were analyzed by PCR genotyping to validate the germ line transmission of the *Mig-6^{LSL}* allele. For genotyping analysis, PCR analysis was used to genotype DNA extracts from tail biopsies (Figure S1 C and D). To detect the *Mig-6^{LSL}* allele (Figure S1), primers P1, P2, and P3 were designed to amplify the fragment from wild type (300 bp) and *Mig-6^{LSL}* allele (450 bp).

Animals and Tissue Collection

Mice were cared for and used in the designated animal care facility according to the Michigan State University institutional guidelines. Mice of various genotypes were sacrificed at 2 and 3 months of age (n=5 per genotype). For the U0126 treatment study, *Pten$^{f/f}$* and *Pten$^{d/d}$* mice at 2 months of age were injected with either vehicle (PBS) or U0126 (50 μmol/kg) for three months (n = 5 per genotype per treatment). Inhibitor injections were repeated every week. After the fourth injection, mice were killed at 5 months of age. Uterine tissues were flash frozen at the time of dissection and stored at −80°C for RNA or fixed with 4% (volume/volume) paraformaldehyde for histology analysis.

Cell Cultures

HeLa, Ishikawa, and 293T were obtained from the American Type Culture Collection (ATCC). Cell lines were maintained in Dulbecco's Modified Eagle Medium supplemented with 10% fetal bovine serum, penicillin, and streptomycin (100 μU/mL). All cells were cultured at 37°C under 5% CO2. All cells were used within 6 months from the time when they were obtained, expanded, and resuscitated from ATCC.

Quantitative real-time PCR

RNA was extracted from the uterine tissues using the RNeasy total RNA isolation kit (Qiagen). RT-PCR was performed using RT-PCR Universal Master Mix reagent (Applied Biosystems) according to the manufacturer's instructions. All RT-PCR Taqman analysis was done by using five independent RNA sets. mRNA quantities were normalized against 18S RNA using ABI rRNA control reagents.

Immunohistochemistry

Uterine sections from paraffin-embedded tissue were cut at 5 μm and mounted on silane-coated slides, deparafinized, and rehydrated in a graded alcohol series. Sections were preincubated with 10% normal serum in PBS (pH 7.5) and then incubated with primary antibody diluted in 10% normal goat serum in PBS (pH 7.5) overnight at 4°C. On the following day, sections were washed in PBS and incubated with a secondary antibody (Vector Laboratories) for 1 hour at room temperature. Immunoreactivity was detected using the Vectastain Elite DAB kit (Vector Laboratories).

Western Blot Analysis

Samples containing 15 μg proteins were applied to SDS-PAGE. The separated proteins were transferred onto a polyvinylidene difluoride membrane (Millipore). Membranes were blocked overnight with 0.5% casein (weight/volume) in PBS with 0.1% Tween 20 (volume/volume) (Sigma Aldrich) and probed with antibodies. Immunoreactivity was visualized by incubation with a horseradish peroxidase-linked secondary antibody and treatment with ECL reagents. To control for loading, the membrane was stripped and probed with anti-Actin (Santa Cruz) and developed again.

Reverse Phase Protein Array (RPPA)

RPPA were performed as previously described (20). Briefly, tissue lysates were printed on nitrocellulose-coated slides and probed with validated antibodies. Signals were captured by tyramide dye deposition (CSA System, DAKO). Data were collected and analyzed using quantification software.

In vitro kinase assay

GST-fusion proteins were incubated with 30 μg of FLAG-MIG-6 transfected cell lysates in the presence of kinase reaction buffer (10 μl 5× kinase buffer, 10 μl magnesium/ATP cocktail solution 90 μl 75 mM MgCl2/500 mM ATP plus 10 μl (100 μCi) of (γ-32P)-ATP (3000 Ci/mmole) in a total volume of 50 μl for 30 min at 30°C. Reactions were terminated by washing twice with 1× kinase buffer. Samples were resuspended in 15 μl 5× SDS sample loading buffer and boiled for 5 min. After electrophoresis, SDS polyacrylamide gels were stained with Coomassie blue and dried, and the phosphorylated products were visualized by autoradiography.

Immunofluorescence analysis

Ishikawa cells were plated at 20 mm glass coverslip and transfected with FLAG-tagged MIG-6 or/and V5-tagged ERK2 plasmids. After incubation for 24 h, cells were fixed for 30 min in cold 4% (weight/volume) paraformaldehyde, and permeabilized for 5 min in 1/40 Triton X-100. Primary antibodies to FLAG (Sigma Aldrich) and V5 (Bethyl Laboratories) were added and overnight at 4°C. After three washes in PBS, coverslips were incubated for 1 h at 37°C with Alexa Fluor 555 donkey anti-rabbit and Alexa Fluor 488 donkey anti-mouse (Invitrogen). Cells were then mounted with mounting media containing 4, 6-diamino-2-phenylindole (Invitrogen) for fluorescence on glass slides and visualized using a Zeiss 510 Meta (NLO) Confocal Microscope (Carl Zeiss).

Duolink in situ proximity ligation assay (PLA) analysis

Duolink in situ PLA analysis was performed according to the manufacturer's instructions (Olink Biosciences). Briefly, paraformaldehyde-fixed cells were washed with PBS, incubated for 10 min in 0.1% (volume/volume) Triton X-100, washed, and blocked with blocking solution. Primary antibodies, against ERK1/2 and Phospho-ERK1/2 antibodies, were applied, and the cells were incubated with PLUS and MINUS secondary PLA probes against rabbit and mouse IgGs. The incubation was followed by hybridization and ligation, and then amplification was performed. After mounting with Duolink mounting medium, samples were examined using a Zeiss 510 Meta (NLO) Confocal Microscope (Carl Zeiss).

Statistical analysis

Statistical analysis was performed with one of following: one-way ANOVA analysis followed by Tukey's post hoc multiple range test, Student's t tests, log-rank test using the Instat package from GraphPad.

Results

Overexpression of *Mig-6* suppresses tumorigenesis in *Pten* deficient endometrial cancer

In order to determine the tumor suppressor function of *Mig-6* in the development of endometrial cancer, we generated conditional overexpression of *Mig-6* mice by using embryonic stem cell targeting on the ROSA26 locus, inserting a CAGGS promoter, loxP-STOP-loxP (LSL) cassette and *Mig-6* cDNA (*Mig-6*^{LSL}). ROSA26 is a locus used for constitutive, ubiquitous gene expression in mice (21). The mouse Rosa26 locus is particularly useful for genetic modification as it can be targeted with high efficiency and is expressed in most cell types tested (22). The CAG promoter is a strong synthetic promoter frequently used to drive high levels of gene expression in mammalian expression vectors (23). Before activation, *Mig-6* is silent due to a floxed STOP cassette inserted between the promoter and the transgene. Upon cre-mediated excision of the STOP cassette, *Mig-6* is constitutively expressed by the ubiquitous CAG promoter. Therefore, this transgenic mouse model can be used to express *Mig-6* in any tissue in a spatial and/or temporal manner if respective cre mouse lines are available (24). *Mig-6*^{LSL} mice were bred to PR-Cre mice (25) to generate *Mig-6* overexpression in the PR-expressing cells (*Mig-6*^{over}; Figure S1 and S2).

Loss of *Pten* (either as a heterozygote or by uterine specific ablation) has been shown to induce endometrial cancer in mice highlighting its important role in endometrial cancer development (7, 26). To assess the effects of the overexpression *Mig-6* on endometrial cancer development and progression, *Mig-6*^{over} mice were bred to the *Pten* floxed (*Pten*$^{f/f}$) mouse model (26) in order to generate ablation of *Pten* and overexpression of *Mig-6* in the uterus (*Mig-6*^{over} *Pten*$^{d/d}$ mice; Figures S2 C and D). *Pten*$^{d/d}$ mice had a decrease survival due to the development of endometrial cancer (26). Therefore, we first examined the survival time of control, *Mig-6*^{over}, *Pten*$^{d/d}$ and *Mig-6*^{over} *Pten*$^{d/d}$ mice. The survival time of *Mig-6*^{over} *Pten*$^{d/d}$ mice was significantly longer than *Pten*$^{d/d}$ mice (Figure 1A). *Mig-6*^{over} *Pten*$^{d/d}$ mice did not die due to the development of endometrial cancer. However, *Pten*$^{d/d}$ mice developed vaginal papillomas as well as endometrial cancer. Overexpression of *Mig-6* did not have a remarkable effect on the vaginal papilloma phenotype of *Pten*$^{d/d}$ mice. The

mice were euthanized if the mice exhibited immobility, inability to eat, >15% weight loss, vaginal prolapse.

To address the impact of overexpression of *Mig-6* on the development and progression of endometrial cancer, control, *Mig-6*^{over}, *Pten*$^{d/d}$ and *Mig-6*^{over} *Pten*$^{d/d}$ mice were sacrificed at 2 and 3 months of age and uterine weight, gross and histological morphology were examined. *Mig-6*^{over} *Pten*$^{d/d}$ mice showed a significant decrease in uterine weight compared to *Pten*$^{d/d}$ mice at 3 months of ages (Figure 1B). Gross morphology at 3 months of age showed that the overexpression of *Mig-6* remarkably suppressed the development of endometrial cancer in *Pten*$^{d/d}$ mice (Figure 1C). Histological analysis demonstrated that the uteri of *Pten*$^{d/d}$ mice exhibited development of endometrial adenocarcinoma at 2 and 3 months of ages as characterized by neoplastic endometrial glands invading through the myometrium (Figure 1D and Figure S3). While endometrial hyperplasia was observed in the uteri of *Mig-6*^{over} *Pten*$^{d/d}$ mice at 2 months, endometrial adenocarcinoma with invasion into the myometrium was not observed (Figure S3). Surprisingly, *Mig-6*^{over} *Pten*$^{d/d}$ mice at 3 months age did not exhibit endometrial hyperplasia (Figure 1D). Additionally, we could not find any pathological effects in *Mig-6*^{over} mice. These results demonstrate that overexpression of *Mig-6* suppresses endometrial cancer progression in conditional uterine ablation of *Pten*.

Overexpression of *Mig-6* inhibits epithelial proliferation in *Pten* deficient endometrial cancer

In order to determine if the suppression of endometrial cancer in *Mig-6*^{over} *Pten*$^{d/d}$ mice is caused by an alteration in cell proliferation, we examined the immunohistochemisry for phospho-histone H3, a mitotic marker. Immunohistochemical analysis showed significantly lower proliferation in uterine epithelial cells of *Mig-6*^{over} *Pten*$^{d/d}$ mice compared to *Pten*$^{d/d}$ mice at 2 months of age (Figures 2A and B). Estrogen-dependent endometrioid carcinoma is the most common type of endometrial cancer (3). Importantly, one of the major pathologic phenomena of an endometrial cancer is the loss of estrogen and progesterone control over uterine epithelial cell proliferation (27). Estrogen rapidly activates the hypoxia-inducible factor 1 alpha (*Hif1* α) (28). The expression of *Hif1* α and its target genes were significantly decreased in *Mig-6*^{over} *Pten*$^{d/d}$ mice compared to the other groups at 3 months of age (Figure 2C).

The expression of PR is increased in *Mig-6*^{over} *Pten*$^{d/d}$

Expressions of PR and ERα have been reported prognostic factors for endometrial carcinoma (29). The expression of PR was increased and its target genes (*Fst* and *Il13ra2*) were significantly increased in uterus of *Mig-6*^{over} *Pten*$^{d/d}$ mice compared to *Pten*$^{d/d}$ mice at 3 months of age (Figures 3A–3C). Expression of ERα itself did not change, but ERα target genes, *Muc-1* and *Ltf*, were significantly decreased in the uterus of *Mig-6*^{over} *Pten*$^{d/d}$ mice at 3 months of age (Figures 3D and Figure S4). These results suggest that overexpression of *Mig-6* suppress endometrial cancer progression by inducing progesterone signaling and suppressing estrogen signaling.

ERK1/2 phosphorylation is highly decreased in *Mig-6^{over} Pten$^{d/d}$* mice

ERK-kinases (MEKs) trigger the activation of ERKs by phosphorylating a threonine and a tyrosine in their activation loop. Specificity in the signaling between these modules is achieved by protein-protein interactions and scaffolding molecules (30). We identified interaction of MIG-6 with ERK2 and demonstrated that ablation of *Mig-6* leads to increased phosphorylation of ERK1/2 (19). Abnormal or constitutive phosphorylation of ERK1/2 leads to tumorigenesis (30). To determine if the decreased tumor formation is related to ERK1/2 signaling in the *Mig-6^{over} Pten$^{d/d}$* uteri, we investigated phosphorylation of ERK1/2 by immunohistochemical analysis. The expression of phospho-ERK1/2 was significantly decreased in *Mig-6^{over} Pten$^{d/d}$* mice compared to *Pten$^{d/d}$* mice at 2 and 3 months of age (Figure 4A). To confirm the increase of ERK1/2 phosphorylation observed by immunostaining in the *Pten$^{d/d}$* uteri, we examined the expression of phospho-ERK1/2 by Western blot analysis in the uteri of *Pten$^{d/d}$ and Mig-6^{over} Pten$^{d/d}$* mice at 2 and 3 months of age. The level of phospho-ERK 1/2 but not total ERK1/2 was increased in the *Pten$^{d/d}$* uteri compared with the *Mig-6^{over} Pten$^{d/d}$* uteri which are consistent with our observations in immunohistochemisry analysis (Figure 4B). Additionally, the expression of ERK1/2 target genes was significantly decreased in *Mig-6^{over} Pten$^{d/d}$* uteri compared to *Pten$^{d/d}$* mice (Figure 4C). ERK1/2 phosphorylates the transcription factor C/EBPβ (31). Consistent with the decreased phospho-ERK1/2, phospho-C/EBPβ but not total C/EBPβ was significantly decreased in *Mig-6^{over} Pten$^{d/d}$* mice compared to *Pten$^{d/d}$* mice at 2 and 3 months of age (Figures S5A and B). PTEN acts as a negative regulator of PI3K signaling, which regulates a number of cellular functions through the activation of AKT (6). The expression of total AKT and phospho-AKT was not altered in endometrium from *Mig-6^{over} Pten$^{d/d}$* mice compared to *Pten$^{d/d}$* mice (Figures S5C and D). These results suggest that the MIG-6 controlled inhibition of ERK1/2 signaling contributes to the decreased rate of tumor formation in *Mig-6^{over} Pten$^{d/d}$* mice.

MIG-6 directly inhibits phosphorylation of ERK1/2 activity

To determine whether MIG-6 physically interacts with ERK2, 293T cells and Ishikawa human endometrial cells were co-transfected with FLAG-MIG-6 and/or ERK2, and then the lysates immunoprecipitated with FLAG antibodies. The immunoprecipitation results showed MIG-6 physically interact with ERK2 (Figure 5A and S6A). Next, we made serial deletions of MIG-6 using PCR amplification of the FLAG-tagged MIG-6 plasmid to determine the ERK2 binding site in MIG-6. The results of in vitro pull-down assays showed that MIG-6 interacts with ERK2 via its SH3 binding domain (Figure S6B). Both MIG-6 and ERK2 proteins were also co-localized in the cytoplasm of Ishikawa cells transfected with FLAG-tagged MIG-6 and/or V5-tagged ERK2 by immunofluorescence analysis (Figure S6C). To determine whether MIG-6 inhibits phosphorylation of ERK2, we performed in vitro kinase assay and Duolink in situ proximity ligation assay (PLA) (32). Overexpression of MIG-6 led to decrease phosphorylation of ERK2 by in vitro kinase assays (Figure 5B). Additionally, we examined the effect of ERK1/2 phosphorylation by MIG-6 overexpression. The overexpression of MIG-6 dose-dependently decreased phosphorylation of ERK1/2 (Figure 5C). Duolink in situ proximity ligation assay (PLA) also showed that MIG-6 overexpression

decreased phosphorylation levels of ERK1/2 (Figure 5D and E). These results suggest that MIG-6 directly inhibits phosphorylation of ERK1/2.

ERK1/2 inhibitor significantly reduces endometrial cancer tumorigenesis in *Pten*$^{d/d}$ mice

To examine whether inhibition of ERK1/2 phosphorylation suppresses tumor progression in endometrial cancer, *Pten*$^{d/d}$ mice were treated with U0126, an effective inhibitor of MAPK/ERK kinase (33). As assessed by immunohistochemistry, phospho-ERK1/2 was markedly reduced in U0126 treated *Pten*$^{d/d}$ mice (Figure 6A). *Pten*$^{d/d}$ mice treated with U0126 exhibited a significant reduction in uterine weight (Figures 6B and C). Histopathological analysis of the entire animal cohort showed that inhibition of ERK1/2 phosphorylation suppressed endometrial cancer progression, as reflected by the arrest of tumors at the hyperplastic or normal stage, whereas tumors from *Pten*$^{d/d}$ mice treated with vehicle advanced to endometrial cancer (Figure 6D). These data suggest that activation of ERK1/2 signaling is critical for endometrial cancer development and progression.

The expression levels between MIG-6 and phospho-ERK1/2 have an inverse correlation in human endometrial cancer

Examination of clinical endometrial specimens showed lower levels of *MIG-6* expression in endometrial cancer with grade I, II and III in comparison to normal endometrium (Figure 7A). To assess the clinical relevance between MIG-6 and phospho-ERK1/2 protein levels in human endometrial carcinoma, we next performed reverse phase protein array (RPPA) consisting of 109 endometrioid carcinoma of the uterine corpus. The correlation studies showed an inverse correlation between MIG-6 and phospho-ERK1/2 in human endometrial cancer (Figures 7B and C). We validated this reverse correlation in endometrial biopsies from patients with endometrioid carcinoma and normal endometrium by immunohistochemistry (Figures 7D).

Discussion

The major pathologic phenomenon of endometrial cancer is the loss of ovarian steroid hormone control over uterine epithelial cell proliferation and apoptosis (34). *Mig-6*, a progesterone signaling mediator, suppresses estrogen signaling in the uterus (16, 35). To determine the tumor suppressor function of *Mig-6* in the development of endometrial cancer, we generated *Mig-6* conditional overexpression mice (*Mig-6*^{over}). To assess the effects of *Mig-6* on the PTEN/PI3K/AKT signaling pathway in uterine tumorigenesis, mice with *Pten* floxed (*Pten*$^{f/f}$) and *Mig-6*^{over} were bred to the PR-Cre mouse model to generate overexpression of *Mig-6* and ablation of *Pten* in the uterus (*Mig-6*^{over} *Pten*$^{d/d}$) (Figure S1 and 2). *Mig-6*^{over} *Pten*$^{d/d}$ mice suppressed to develop endometrial cancer (Figure 1). The ablation of both *Mig-6* and *Pten* dramatically accelerated the development of endometrial cancer compared to single ablation of either gene (19). Thus, these results demonstrate the importance of *Mig-6* in human endometrial cancer.

Proliferations in epithelial cells were significant decreased in *Mig-6*^{over} *Pten*$^{d/d}$ mice compared to *Pten*$^{d/d}$ mice (Figures 2A and B). Regions of hypoxia are reported to exist within many tumors, and the extent of tumor hypoxia correlates with prognosis in number

types (36). In addition, increased levels of HIF1α protein have been detected in the cytoplasm and nuclei of 40% to 80% of human carcinoma cases (36). To determine if overexpressed *Mig-6* regulates uterine epithelial proliferation suppressing HIF1α singling, we determined transcription levels of *Hif1a* and its target genes. These genes were significantly decreased in *Mig-6*^{over} *Pten*$^{d/d}$ mice compared to *Pten*$^{d/d}$ mice (Figure 2C). These results indicate that a decrease of proliferation lead to retard the endometrial cancer development and progression in *Mig-6*^{over} *Pten*$^{d/d}$ mice via regulating HIF1α signaling.

We evaluated the expression of PR and ERα by immunohistochemistry. PR protein level in stromal cells and PR targets (*Il13ra2* and *Fst*) were highly increased in *Mig-6*^{over} *Pten*$^{d/d}$ mice compared to *Pten*$^{d/d}$ mice at 3 months of age (Figure 3C). ERα protein level was not changed between *Pten*$^{d/d}$ and *Mig-6*^{over} *Pten*$^{d/d}$ mice. However, ERα target genes, *Muc-1* and *Ltf* expression were highly decreased in *Mig-6*^{over} *Pten*$^{d/d}$ mice compared to *Pten*$^{d/d}$ mice (Figure 3D and Figure S4). Our results suggest that overexpression of *Mig-6* suppress endometrial cancer progression by inducing P4 signaling and suppressing E2 signaling.

Reduced PR expression was observed in human endometrial cancer (29). Expression of PR is essential for uterine biology (27). In addition, expression of PR and ERα is linked because transcription of the PR gene is induced by estrogen and inhibited by progestins (37). *Mig-6* is a downstream target of PR and EGF (16). Conditional ablation of *Mig-6* in the uterus leads to the development of endometrial hyperplasia and estrogen-induced endometrial cancer. Interestingly, conditional ablation of *Mig-6* in uterus resulted in reduced PR expression in stromal cells as also seen in human endometrial cancer (18) and overexpression of *Mig-6* induced PR expression in *Pten* mutation (Figure 3A and B). The regulation of PR expression in the endometrial epithelial and stromal cells by *Mig-6* is critical for the ability of P4 to attenuate the E2 regulated proliferation, apoptosis and expression of ERα target genes. It has been reported that PR is essential for uterine biology as a key regulator of uterine epithelial-stromal crosstalk (38). The expression of PR is significantly decreased by siEGFR in uterine stromal cells (39). It has been reported that EGFR ligands, *Hbegf* and *Areg*, as well as *Egfr* itself, are PR target genes (40). An attractive conjecture would be that a feed-forward amplification loop exists in which PR induces EGFR/ERK signaling that in turn feeds back to maintain PR activation. Such a model would serve as an exquisite sensor of P4 activity.

Estrogen-mediated induction of the majority of signaling pathways leads to the activation of two key signaling cascades, the PTEN/PI3K/AKT and the ERK pathways (41). The estrogen receptors mediate the effect of estrogen under physiological and pathological conditions either by activation of estrogen target genes transcription by binding to specific estrogen response elements (42) or *via* nongenomic mechanisms which results in the rapid activation of several signal transduction pathways to regulate different cellular processes, such as proliferation, apoptosis, and differentiation. Estrogen exerts a proliferative effect *via* non-genomic activation of ERK1/2 and PI3K/AKT (43). To determine whether overexpressed *Mig-6* regulate ERK1/2 phosphorylation in PTEN-null endometrial cancer, we assessed the expression of phospho-ERK1/2 by immunohistochemistry and Western blot. The expression of phospho-ERK1/2 and its target genes was significantly decreased in *Mig-6*^{over} *Pten*$^{d/d}$

mice compared to *Pten*$^{d/d}$ mice. However, the PTEN/PI3K/AKT pathways related proteins were not changed between *Pten*$^{d/d}$ and *Mig-6*^{over} *Pten*$^{d/d}$ mice (Figure S5).

Mig-6 only decreases ERK downstream genes in *Mig-6*^{over}*Pten*$^{d/d}$ mice, not in *Mig-6*^{over} mice (Figure 4). ERK1/2 signaling is known to regulate cell proliferation and apoptosis in uterine endometrial cells. Aberrant activation of ERK1/2 has been implicated in the pathological processes of endometrial cancer (44). ERK1/2 is critical for decidualization during early pregnancy (45). However, ERK1/2 signaling is not activated in non-pregnant uteri. *Mig-6* is a negative regulator of EGFR-ERK signaling (46). While there was a slight decrease of *Serpine* and *F3* expression in *Mig-6*^{over} mice compared to control mice, it was not significant. Therefore, ERK downstream genes are not significantly changed in *Mig-6*^{over} mice compared to control mice.

We have identified that MIG-6 interacts with ERK2 (19). Therefore, we examined whether MIG-6 directly affects ERK1/2 phosphorylation. Protein interaction between MIG-6 and ERK1/2 was observed by immunoprecipitation and immunofluorescence analysis in transiently co-transfected cells with MIG-6 and/or ERK2 and GST pull-down assay using in vitro-translated MIG-6 proteins and GST-fused ERK2 protein (Figures S6). In vitro kinase assays using GST-ERK2 proteins and western blot analysis using the phosphorylated ERK1/2 antibody showed that MIG-6 overexpression decreased phosphorylation of ERK1/2 (Figures 5B and C). Additionally, proximity ligation assay using the Duolink in situ PLA kit also showed that MIG-6 overexpression decreased levels of phospho-ERK2 (Figures 5D and E). These results demonstrate that MIG-6 directly inhibits phosphorylation of ERK1/2. MAPK/ERK-kinases (MEKs) trigger the activation of ERKs by phosphorylating a threonine and a tyrosine in their activation loop (30). U0126 is highly selective inhibitors of ERK signaling (33). *Pten*$^{d/d}$ mice showed significantly reduced endometrial tumorigenesis after U0126 treatment (Figure 6). *Pten*$^{d/d}$ mice treated with U0126 exhibited a significant reduction in uterine weight. Histopathological analysis of the entire animal cohort showed that inhibition of ERK1/2 phosphorylation suppressed endometrial cancer progression to hyperplasia or normal stage in *Pten*$^{d/d}$ mice. These findings suggest that regulation of ERK1/2 phosphorylation is important for the progression of PTEN-mutant endometrial cancer.

To determine the clinical relevance of MIG-6 and ERK1/2 in human, we performed reverse phase protein array (RPPA). RPPA is a recently developed quantitative assay that analyzes nanoliter amounts of sample for potentially hundreds of proteins (20). We revealed the significance of MIG-6 in human endometrial cancer through sample analysis, where MIG-6 expression is inversely associated with ERK1/2 phosphorylation (Figure 7). These results suggest that aberrant overexpression of ERK1/2 phorphorylation is important for a tumor development and progression in mouse as well as human. ERK1/2 is a potential drug target for the intervention of human endometrial cancer.

MIG-6 acts as a negative feedback regulator of EGFR (47). Its transcription is induced by the ERK pathway that is activated by growth factors such as EGF (14). MIG-6 has several functional motifs/domains that are crucial for interaction with other signaling molecules (35, 48). MIG-6 binds to the tyrosine kinase domains of EGFR and ErbB2 and inhibits the

tyrosine kinase activity. We have identified a novel interaction of MIG-6 with ERK (Figures 5 and S6). MAPK/ERK-kinases (MEKs) trigger the activation of ERKs by phosphorylating a threonine and a tyrosine in their activation loop. Specificity in the signaling between these modules is achieved by protein-protein interactions and scaffolding molecules (30). These results suggest that MIG-6 also acts as a negative feedback regulator of ERK. MIG-6 interaction with ERK may suppress ERK phosphorylation by competing MEK interaction.

PTEN regulates several signaling pathways, such as phosphoinositide 3- kinase (PI3K)/ protein kinase B (AKT), janus kinase (JAK)/signal transducers and activators of transcription (STAT), focal adhesion kinase (FAK), and ERK1/2, where activation of these pathways typically leads to cancer development and progression (49). Our results demonstrate that *Mig-6* suppresses tumorigenesis in the uterus of *Pten*-mutation mice by inhibiting ERK1/2 phosphorylation. PR directly interacts with STAT3 through protein-protein interactions in uterus (50). Our previous study showed that activated stromal *Mig-6* by P4 prevented development of endometrial hyperplasia via PR and STAT3 signaling (18). These data suggest that regulation of STAT3 and PR crosstalk is important for endometrial hyperplasia and cancer development.

Loss of PTEN, and subsequent Akt activation, resulted in the activation of ERα-dependent pathways that play an important role in the tumorigenesis of endometrial cancer. The PTEN/ PI3K/AKT signaling pathway can also be activated by E2 and growth factors, suggesting a cross-talk between PTEN/PI3K/AKT and EGFR/MAPK signaling pathways. E2 leads activation of EGFR-ERK signaling (8) and *Mig-6* is mainly known to be a negative regulator of EGFR-ERK signaling through direct interaction with the EGFR family (46). Previously, we demonstrated that the absence of *Mig-6* in mice results in the inability of P4 to inhibit E2-induced uterine weight gain and expression of E2-responsive target genes (16). *Mig-6*, a progesterone target gene, directly interacts with ERK2 and inhibits the phosphorylation of ERK1/2 (19). Phospho-ERK1/2 was significantly decreased in the endometrium of $Mig\text{-}6^{over}Pten^{d/d}$ mice compared to $Pten^{d/d}$ mice (Figure 4). ERK inhibitor treatment significantly reduced endometrial cancer tumorigenesis in $Pten^{d/d}$ mice (Figure 6). This data suggests that aberrant activation of ERK signaling is critical for cancer development and progression in PTEN-deficient cancer. Our findings highlight a crucial tumor suppressor role for *Mig-6* in the progression of PTEN-null endometrial cancer by inhibiting ERK1/2 phosphorylation. *Mig-6* is a mediator of progesterone signaling, and its activity can suppress unopposed-estrogen signaling. Therefore, our studies provide a potential new drug target for the intervention of metastatic human endometrial cancer.

Supplementary Material

Refer to Web version on PubMed Central for supplementary material.

Acknowledgments

We would like to thank Dr. Francesco J. DeMayo for helpful discussion. The $Pten^{f/f}$ mice were acquired from Dr. Hong Wu (University of California, Los Angeles, Los Angeles, CA). This work was supported in part by NIH Grant 5R01HD057873 and America Cancer Society, RSG-12-084-01-TBG to J.W.J. and the National Research Foundation of Korea (NRF) grant funded by the Korea Government (MSIP) (No. NRF-2012R1A2A1A01001862 and NRF-2011-0030086) to H.G.Y.

References

1. Di Cristofano A, Ellenson LH. Endometrial Carcinoma. Annu Rev Pathol. 2007; 2:57–85. [PubMed: 18039093]
2. Siegel R, Naishadham D, Jemal A. Cancer statistics, 2013. CA: a cancer journal for clinicians. 2013; 63:11–30. [PubMed: 23335087]
3. Ziel HK, Finkle WD. Increased risk of endometrial carcinoma among users of conjugated estrogens. N Engl J Med. 1975; 293:1167–70. [PubMed: 171569]
4. Steck PA, Pershouse MA, Jasser SA, Yung WK, Lin H, Ligon AH, et al. Identification of a candidate tumour suppressor gene, MMAC1, at chromosome 10q23.3 that is mutated in multiple advanced cancers. Nat Genet. 1997; 15:356–62. [PubMed: 9090379]
5. Levine RL, Cargile CB, Blazes MS, van Rees B, Kurman RJ, Ellenson LH. PTEN mutations and microsatellite instability in complex atypical hyperplasia, a precursor lesion to uterine endometrioid carcinoma. Cancer Res. 1998; 58:3254–8. [PubMed: 9699651]
6. Vivanco I, Sawyers CL. The phosphatidylinositol 3-Kinase AKT pathway in human cancer. Nat Rev Cancer. 2002; 2:489–501. [PubMed: 12094235]
7. Vilgelm A, Lian Z, Wang H, Beauparlant SL, Klein-Szanto A, Ellenson LH, et al. Akt-mediated phosphorylation and activation of estrogen receptor alpha is required for endometrial neoplastic transformation in Pten+/− mice. Cancer Res. 2006; 66:3375–80. [PubMed: 16585156]
8. Chambliss KL, Yuhanna IS, Anderson RG, Mendelsohn ME, Shaul PW. ERbeta has nongenomic action in caveolae. Mol Endocrinol. 2002; 16:938–46. [PubMed: 11981029]
9. Huet-Hudson YM, Andrews GK, Dey SK. Cell type-specific localization of c-myc protein in the mouse uterus: modulation by steroid hormones and analysis of the periimplantation period. Endocrinology. 1989; 125:1683–90. [PubMed: 2667965]
10. Jick SS. Combined estrogen and progesterone use and endometrial cancer. Epidemiology. 1993; 4:384. [PubMed: 8347751]
11. Minaguchi T, Nakagawa S, Takazawa Y, Nei T, Horie K, Fujiwara T, et al. Combined phospho-Akt and PTEN expressions associated with post-treatment hysterectomy after conservative progestin therapy in complex atypical hyperplasia and stage Ia, G1 adenocarcinoma of the endometrium. Cancer Lett. 2007; 248:112–22. [PubMed: 16919866]
12. Ehrlich CE, Young PC, Stehman FB, Sutton GP, Alford WM. Steroid receptors and clinical outcome in patients with adenocarcinoma of the endometrium. Am J Obstet Gynecol. 1988; 158:796–807. [PubMed: 2966586]
13. Decruze SB, Green JA. Hormone therapy in advanced and recurrent endometrial cancer: a systematic review. International journal of gynecological cancer : official journal of the International Gynecological Cancer Society. 2007; 17:964–78. [PubMed: 17442022]
14. Makkinje A, Quinn DA, Chen A, Cadilla CL, Force T, Bonventre JV, et al. Gene 33/Mig-6, a transcriptionally inducible adapter protein that binds GTP-Cdc42 and activates SAPK/JNK. A potential marker transcript for chronic pathologic conditions, such as diabetic nephropathy. Possible role in the response to persistent stress. J Biol Chem. 2000; 275:17838–47. [PubMed: 10749885]
15. Zhang YW, Staal B, Su Y, Swiatek P, Zhao P, Cao B, et al. Evidence that MIG-6 is a tumor-suppressor gene. Oncogene. 2006
16. Jeong JW, Lee HS, Lee KY, White LD, Broaddus RR, Zhang YW, et al. Mig-6 modulates uterine steroid hormone responsiveness and exhibits altered expression in endometrial disease. Proceedings of the National Academy of Sciences of the United States of America. 2009; 106:8677–82. [PubMed: 19439667]
17. Amatschek S, Koenig U, Auer H, Steinlein P, Pacher M, Gruenfelder A, et al. Tissue-wide expression profiling using cDNA subtraction and microarrays to identify tumor-specific genes. Cancer Res. 2004; 64:844–56. [PubMed: 14871811]
18. Kim TH, Lee DK, Cho SN, Orvis GD, Behringer RR, Lydon JP, et al. Critical tumor suppressor function mediated by epithelial Mig-6 in endometrial cancer. Cancer Res. 2013; 73:5090–9. [PubMed: 23811943]

19. Kim TH, Franco HL, Jung SY, Qin J, Broaddus RR, Lydon JP, et al. The synergistic effect of Mig-6 and Pten ablation on endometrial cancer development and progression. Oncogene. 2010; 29:3770–80. [PubMed: 20418913]
20. Iadevaia S, Lu Y, Morales FC, Mills GB, Ram PT. Identification of optimal drug combinations targeting cellular networks: integrating phospho-proteomics and computational network analysis. Cancer Res. 2010; 70:6704–14. [PubMed: 20643779]
21. Kisseberth WC, Brettingen NT, Lohse JK, Sandgren EP. Ubiquitous expression of marker transgenes in mice and rats. Developmental biology. 1999; 214:128–38. [PubMed: 10491262]
22. Irion S, Luche H, Gadue P, Fehling HJ, Kennedy M, Keller G. Identification and targeting of the ROSA26 locus in human embryonic stem cells. Nature biotechnology. 2007; 25:1477–82.
23. Alexopoulou AN, Couchman JR, Whiteford JR. The CMV early enhancer/chicken beta actin (CAG) promoter can be used to drive transgene expression during the differentiation of murine embryonic stem cells into vascular progenitors. BMC cell biology. 2008; 9:2. [PubMed: 18190688]
24. Wu SP, Lee DK, Demayo FJ, Tsai SY, Tsai MJ. Generation of ES cells for conditional expression of nuclear receptors and coregulators in vivo. Mol Endocrinol. 2010; 24:1297–304. [PubMed: 20382891]
25. Soyal SM, Mukherjee A, Lee KY, Li J, Li H, DeMayo FJ, et al. Cre-mediated recombination in cell lineages that express the progesterone receptor. Genesis. 2005; 41:58–66. [PubMed: 15682389]
26. Daikoku T, Hirota Y, Tranguch S, Joshi AR, DeMayo FJ, Lydon JP, et al. Conditional loss of uterine Pten unfailingly and rapidly induces endometrial cancer in mice. Cancer Res. 2008; 68:5619–27. [PubMed: 18632614]
27. Franco HL, Jeong JW, Tsai SY, Lydon JP, DeMayo FJ. In vivo analysis of progesterone receptor action in the uterus during embryo implantation. Semin Cell Dev Biol. 2008; 19:178–86. [PubMed: 18280760]
28. Semenza GL. Hypoxia-inducible factor 1: oxygen homeostasis and disease pathophysiology. Trends in molecular medicine. 2001; 7:345–50. [PubMed: 11516994]
29. Nyholm HC, Nielsen AL, Lyndrup J, Dreisler A, Thorpe SM. Estrogen and progesterone receptors in endometrial carcinoma: comparison of immunohistochemical and biochemical analysis. Int J Gynecol Pathol. 1993; 12:246–52. [PubMed: 7688353]
30. Kolch W. Coordinating ERK/MAPK signalling through scaffolds and inhibitors. Nat Rev Mol Cell Biol. 2005; 6:827–37. [PubMed: 16227978]
31. Park JS, Qiao L, Gilfor D, Yang MY, Hylemon PB, Benz C, et al. A role for both Ets and C/EBP transcription factors and mRNA stabilization in the MAPK-dependent increase in p21 (Cip-1/WAF1/mda6) protein levels in primary hepatocytes. Mol Biol Cell. 2000; 11:2915–32. [PubMed: 10982390]
32. Koos B, Andersson L, Clausson CM, Grannas K, Klaesson A, Cane G, et al. Analysis of Protein Interactions in situ by Proximity Ligation Assays. Current topics in microbiology and immunology. 2013
33. Favata MF, Horiuchi KY, Manos EJ, Daulerio AJ, Stradley DA, Feeser WS, et al. Identification of a novel inhibitor of mitogen-activated protein kinase kinase. J Biol Chem. 1998; 273:18623–32. [PubMed: 9660836]
34. Sherman ME, Sturgeon S, Brinton LA, Potischman N, Kurman RJ, Berman ML, et al. Risk factors and hormone levels in patients with serous and endometrioid uterine carcinomas. Mod Pathol. 1997; 10:963–8. [PubMed: 9346174]
35. Kim TH, Lee DK, Franco HL, Lydon JP, Jeong JW. ERBB receptor feedback inhibitor 1 regulation of estrogen receptor activity is critical for uterine implantation in mice. Biology of reproduction. 2010; 82:706–13. [PubMed: 20018910]
36. Zhong H, De Marzo AM, Laughner E, Lim M, Hilton DA, Zagzag D, et al. Overexpression of hypoxia-inducible factor 1alpha in common human cancers and their metastases. Cancer Res. 1999; 59:5830–5. [PubMed: 10582706]

37. Savouret JF, Chauchereau A, Misrahi M, Lescop P, Mantel A, Bailly A, et al. The progesterone receptor. Biological effects of progestins and antiprogestins. Hum Reprod. 1994; 9 (Suppl 1):7–11. [PubMed: 7962473]
38. Cunha GR, Cooke PS, Kurita T. Role of stromal-epithelial interactions in hormonal responses. Archives of histology and cytology. 2004; 67:417–34. [PubMed: 15781983]
39. Large MJ, Wetendorf M, Lanz RB, Hartig SM, Creighton CJ, Mancini MA, et al. The Epidermal Growth Factor Receptor Critically Regulates Endometrial Function during Early Pregnancy. PLoS genetics. 2014; 10:e1004451. [PubMed: 24945252]
40. Rubel CA, Lanz RB, Kommagani R, Franco HL, Lydon JP, DeMayo FJ. Research resource: Genome-wide profiling of progesterone receptor binding in the mouse uterus. Mol Endocrinol. 2012; 26:1428–42. [PubMed: 22638070]
41. Cheskis BJ, Greger J, Cooch N, McNally C, McLarney S, Lam HS, et al. MNAR plays an important role in ERa activation of Src/MAPK and PI3K/Akt signaling pathways. Steroids. 2008; 73:901–5. [PubMed: 18261753]
42. Acconcia F, Kumar R. Signaling regulation of genomic and nongenomic functions of estrogen receptors. Cancer Lett. 2006; 238:1–14. [PubMed: 16084012]
43. Boland R, Vasconsuelo A, Milanesi L, Ronda AC, de Boland AR. 17beta-estradiol signaling in skeletal muscle cells and its relationship to apoptosis. Steroids. 2008; 73:859–63. [PubMed: 18272190]
44. Roskoski R Jr. ERK1/2 MAP kinases: structure, function, and regulation. Pharmacol Res. 2012; 66:105–43. [PubMed: 22569528]
45. Lee CH, Kim TH, Lee JH, Oh SJ, Yoo JY, Kwon HS, et al. Extracellular signal-regulated kinase 1/2 signaling pathway is required for endometrial decidualization in mice and human. PloS one. 2013; 8:e75282. [PubMed: 24086495]
46. Ferby I, Reschke M, Kudlacek O, Knyazev P, Pante G, Amann K, et al. Mig6 is a negative regulator of EGF receptor-mediated skin morphogenesis and tumor formation. Nat Med. 2006; 12:568–73. [PubMed: 16648858]
47. Zhang X, Pickin KA, Bose R, Jura N, Cole PA, Kuriyan J. Inhibition of the EGF receptor by binding of MIG6 to an activating kinase domain interface. Nature. 2007; 450:741–4. [PubMed: 18046415]
48. Zhang YW, Vande Woude GF. Mig-6, signal transduction, stress response and cancer. Cell cycle. 2007; 6:507–13. [PubMed: 17351343]
49. Chetram MA, Hinton CV. PTEN regulation of ERK1/2 signaling in cancer. Journal of receptor and signal transduction research. 2012; 32:190–5. [PubMed: 22737980]
50. Lee JH, Kim TH, Oh SJ, Yoo JY, Akira S, Ku BJ, et al. Signal transducer and activator of transcription-3 (Stat3) plays a critical role in implantation via progesterone receptor in uterus. FASEB journal : official publication of the Federation of American Societies for Experimental Biology. 2013; 27:2553–63. [PubMed: 23531596]

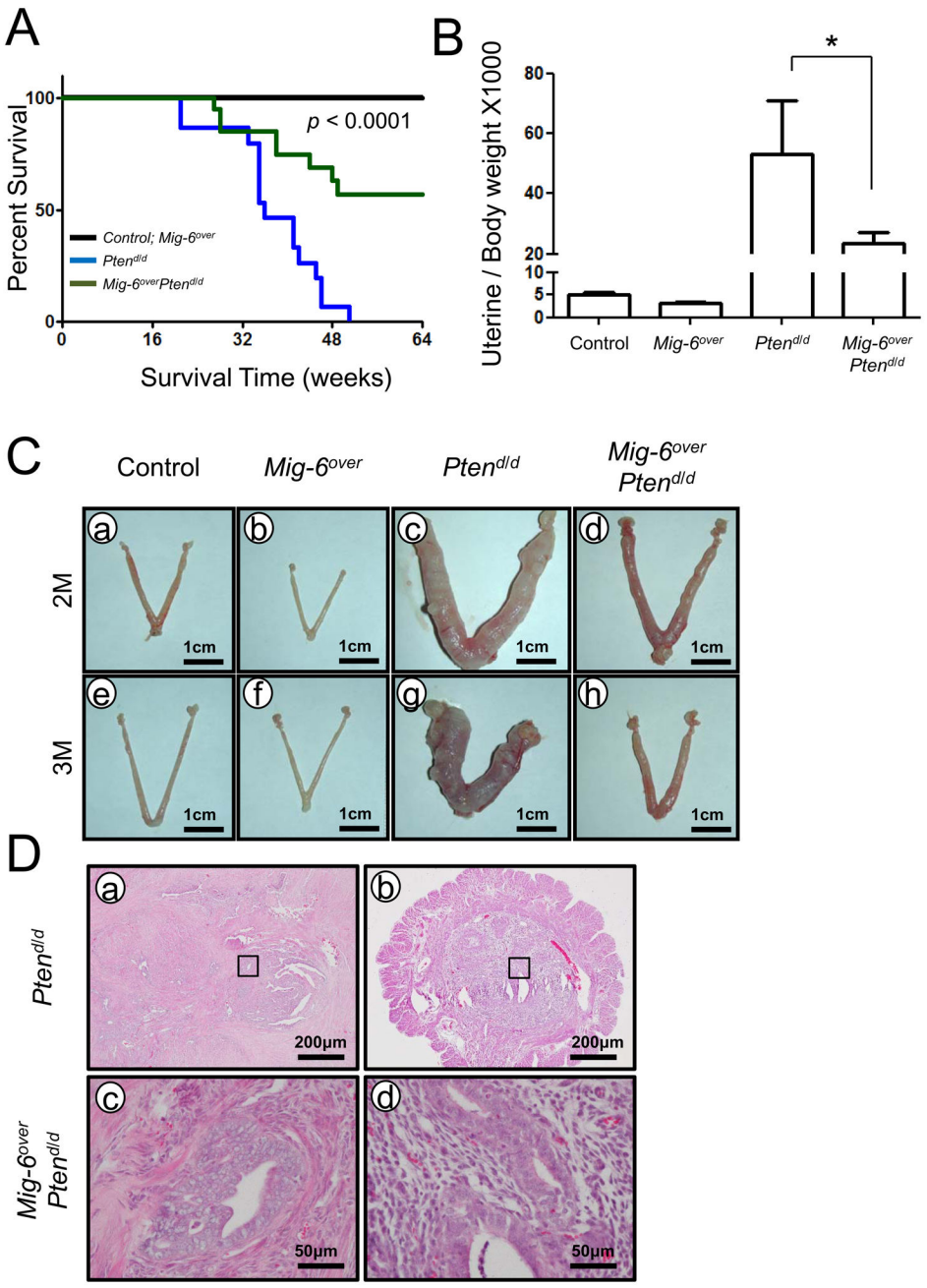

Figure 1.

Overexpression of *Mig-6* retards endometrial cancer progression in conditional uterine ablation of *Pten*. (A) *Mig-6*^{over}*Pten*$^{d/d}$ mice exhibit significantly increased survival time. Survival time in control (black), *Mig-6*^{over} (black), *Pten*$^{d/d}$ (blue), and *Mig-6*^{over}*Pten*$^{d/d}$ (green) mice. $p<0.0001$ (between *Pten*$^{d/d}$ and *Mig-6*^{over}*Pten*$^{d/d}$), n=20 per genotype. (B) The ratio of uterine weight to body weight in control, *Mig-6*^{over}*Pten*$^{d/d}$, *Pten*$^{d/d}$ and *Mig-6*^{over}*Pten*$^{d/d}$ mice at 3 months of age. The results represent the mean ± SEM. * $p<0.05$. (C) The uterine morphology in Control, *Mig-6*^{over}, *Pten*$^{d/d}$ and *Mig-6*^{over}*Pten*$^{d/d}$ mice at 2

months of age (a, b, c and d) and 3 months of age (e, f, g and h). (D) H&E staining of *Pten*$^{d/d}$ *a*nd *Mig-6*^{over}*Pten*$^{d/d}$ mice at 3 months of age.

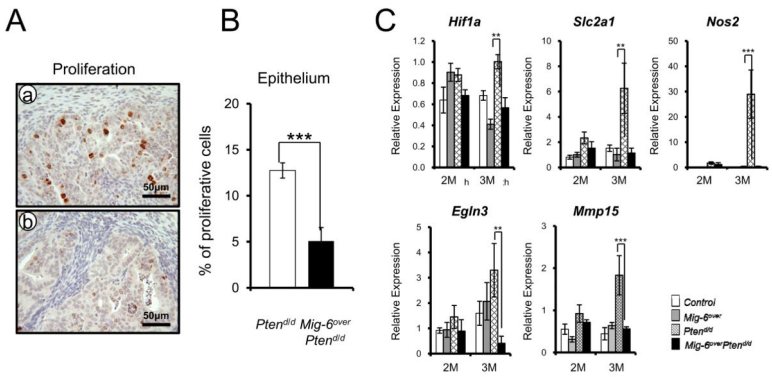

Figure 2.

The regulation of proliferation and apoptosis by *Mig-6* overexpression when *Pten* is mutated. (A) Immunohistochemical analysis of phospho-histone H3 as a proliferation marker in uteri of $Pten^{d/d}$ (a) and $Mig\text{-}6^{over}Pten^{d/d}$ (b) mice at 2 months of age. (B) Quantification of phospho-histone H3 positive cells in epithelial cells. (C) The regulation of the hypoxia-inducible factor 1 in $Mig\text{-}6^{over}Pten^{d/d}$ mice. Real-time RT-PCR analysis of *Hif1a, Slc2a1, Nos2, Egln3,* and *Mmp15* was performed on uteri of from control, $Mig\text{-}6^{over}$, $Pten^{d/d}$ and $Mig\text{-}6^{over}Pten^{d/d}$ mice at 2 and 3 months of age. The results represent the mean ± SEM. * $p<0.05$, ** $p<0.01$, *** $p<0.001$.

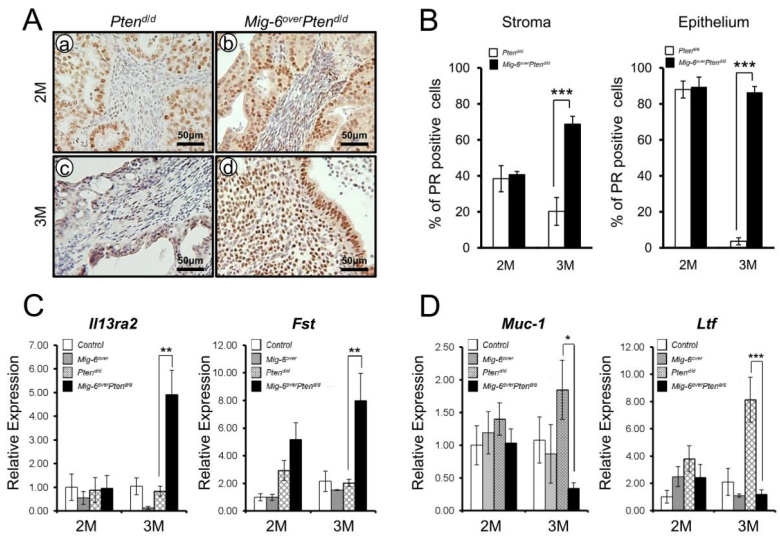

Figure 3.

The expression of PR is recovered in *Mig-6*^{over}*Pten*$^{d/d}$. (A) Immunohistochemical analysis of PR in the uteri of *Pten*$^{d/d}$ and *Mig-6*^{over}*Pten*$^{d/d}$ mice at 2 (a and b) and 3 (c and d) months of age. (B) Quantification of PR positive cells in the uteri of *Pten*$^{d/d}$ and *Mig-6*^{over}*Pten*$^{d/d}$ mice. (C) The expression of PR target genes. Real-time RT-PCR analysis of *Il13ra2* and *Fst* was performed on uteri of control, *Mig-6*^{over}, *Pten*$^{d/d}$ and *Mig-6*^{over}*Pten*$^{d/d}$ mice at 2 and 3 months of age. (D) The expression of ERα target genes. Real-time RT-PCR analysis of *Muc-1* and *Ltf* was performed on uteri of from control, *Mig-6*^{over}, *Pten*$^{d/d}$ and *Mig-6*^{over}*Pten*$^{d/d}$ mice at 2 and 3 months of age. The results represent the mean ± SEM. * $p<0.05$, ** $p<0.01$, *** $p<0.001$.

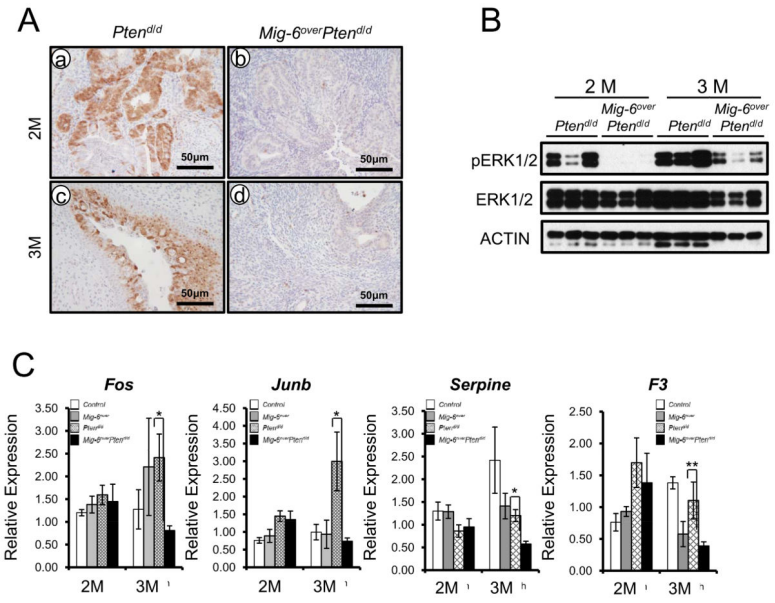

Figure 4.

The expression of phospho-ERK1/2 is significantly reduced in *Mig-6*^{over}*Pten*$^{d/d}$ mice. (A) Immunohistochemical analysis of phospho-ERK1/2 in the uteri of *Pten*$^{d/d}$ *a*nd *Mig-6*^{over}*Pten*$^{d/d}$ mice at 2 (a and b) and 3 (c and d) months of age. (B) Western blot analysis of phospho-ERK1/2, ERK1/2, and ACTIN in the uteri of *Pten*$^{d/d}$ and *Mig-6*^{over}*Pten*$^{d/d}$ mice at 2 and 3 months of age. Equal amounts of protein were subjected to SDS-PAGE and Western blot analysis. (C) The expression of ERK1/2 target genes. Real-time RT-PCR analysis of *Fos*, *Junb*, *Serpine* and *F3* was performed on uteri of from control, *Mig-6*^{over}, *Pten*$^{d/d}$ and *Mig-6*^{over}*Pten*$^{d/d}$ mice at 2 and 3 months of age. The results represent the mean ± SEM. * $p<0.05$, ** $p<0.01$.

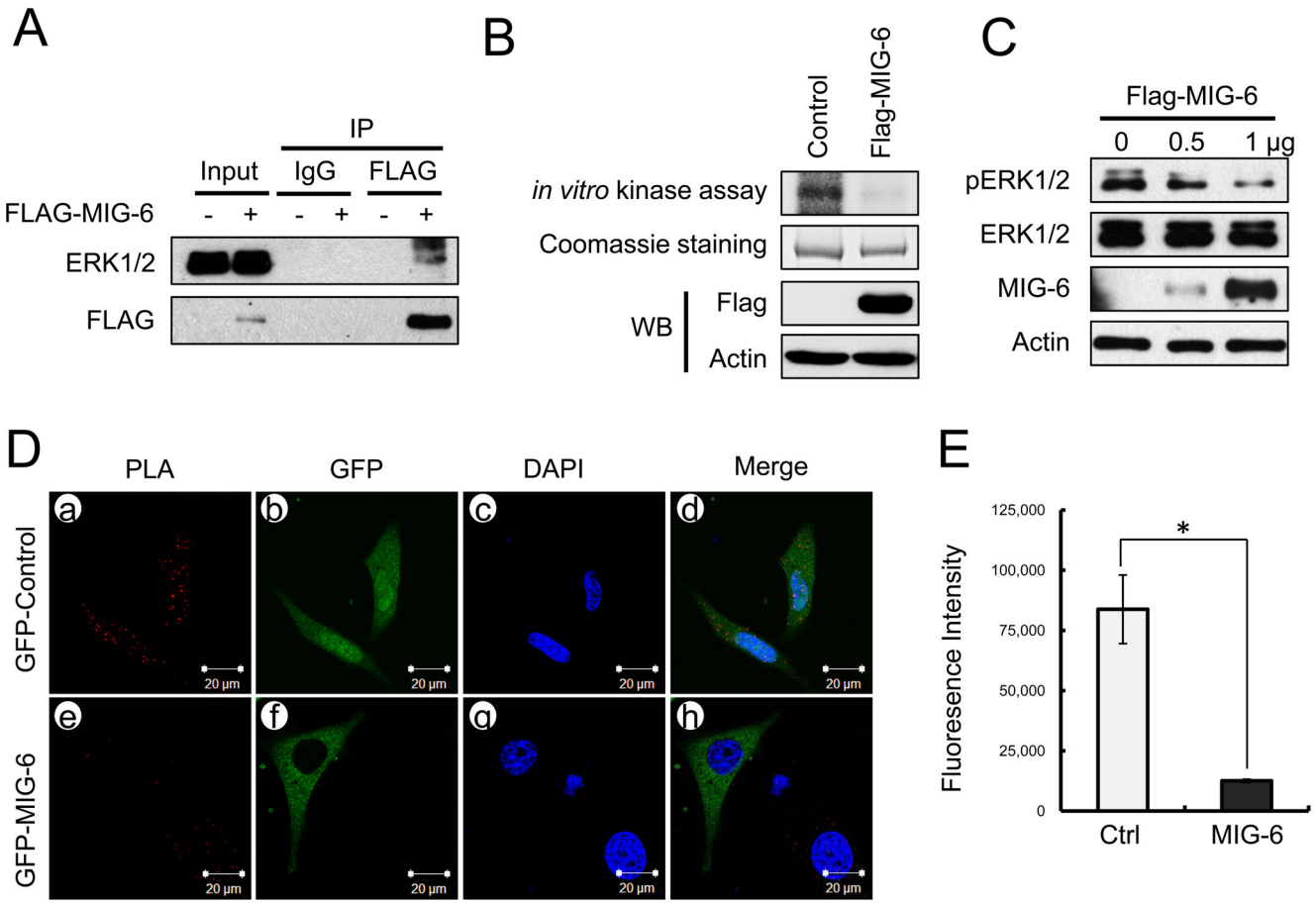

Figure 5.

MIG-6 deregulates ERK1/2 activity. (A) The protein interaction between MIG-6 and ERK1/2 by immunoprecipitation and Western blot analysis in FLAG-tagged MIG-6 transfected Ishikawa cells. (B) In vitro kinase assays were performed with FLAG-tagged MIG-6 transfected HeLa cell lysates and the GST-fused ERK2 proteins in kinase reaction buffer. Phosphorylated products were eluted and visualized by autoradiography. (C) Flag-tagged MIG-6 transfected Ishikawa cell lysates as dose-dependent manner were analyzed by Western blotting. (D) For the Duolink in situ PLA analysis, HeLa cells were transfected with GFP-control (a, b, c and d) and the GFP-tagged MIG-6 (e, f, g and h) plasmids. The level of ERK1/2 phosphorylation was assessed with ERK1/2 antibody and phospho-ERK1/2 antibody. The positive signal was analyzed using confocal microscopy. (E) Intensity of PLA analysis was obtained using Image J software. MIG-6 overexpressed cells display decreased fluorescence intensity compared to untransfected cells. The results represent the mean ± SEM. * $p<0.05$

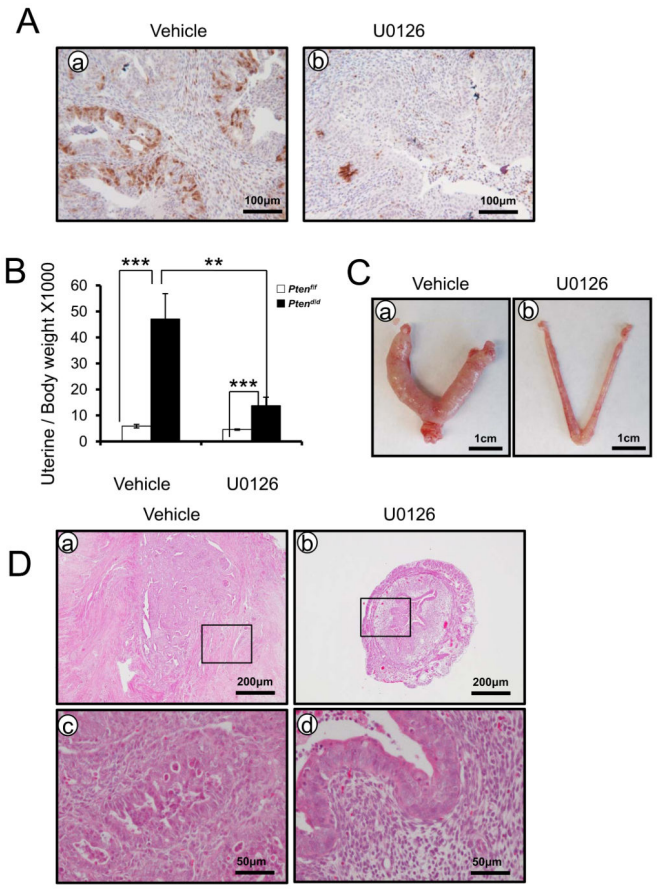

Figure 6.

MAPK/ERK signaling is critical for endometrial cancer progression and development. (A) Immunohistochemical analysis of phospho-ERK1/2 in the uteri of *Pten*$^{d/d}$ mice treated with vehicle (a) and U0126 (b). (B) *Pten*$^{d/d}$ mice treated with U0126 shows decreased uterine weight compared with *Pten*$^{d/d}$ mice treated with vehicle. The results represent the mean ± SEM. *** $p<0.001$, ** $p<0.01$. (C) Gross morphology of *Pten*$^{d/d}$ mice treated with vehicle (a) and U0126 (b). (D) Hematoxylin-eosin staining of *Pten*$^{d/d}$ mice treated with vehicle (a and c) and U0126 (b and d).

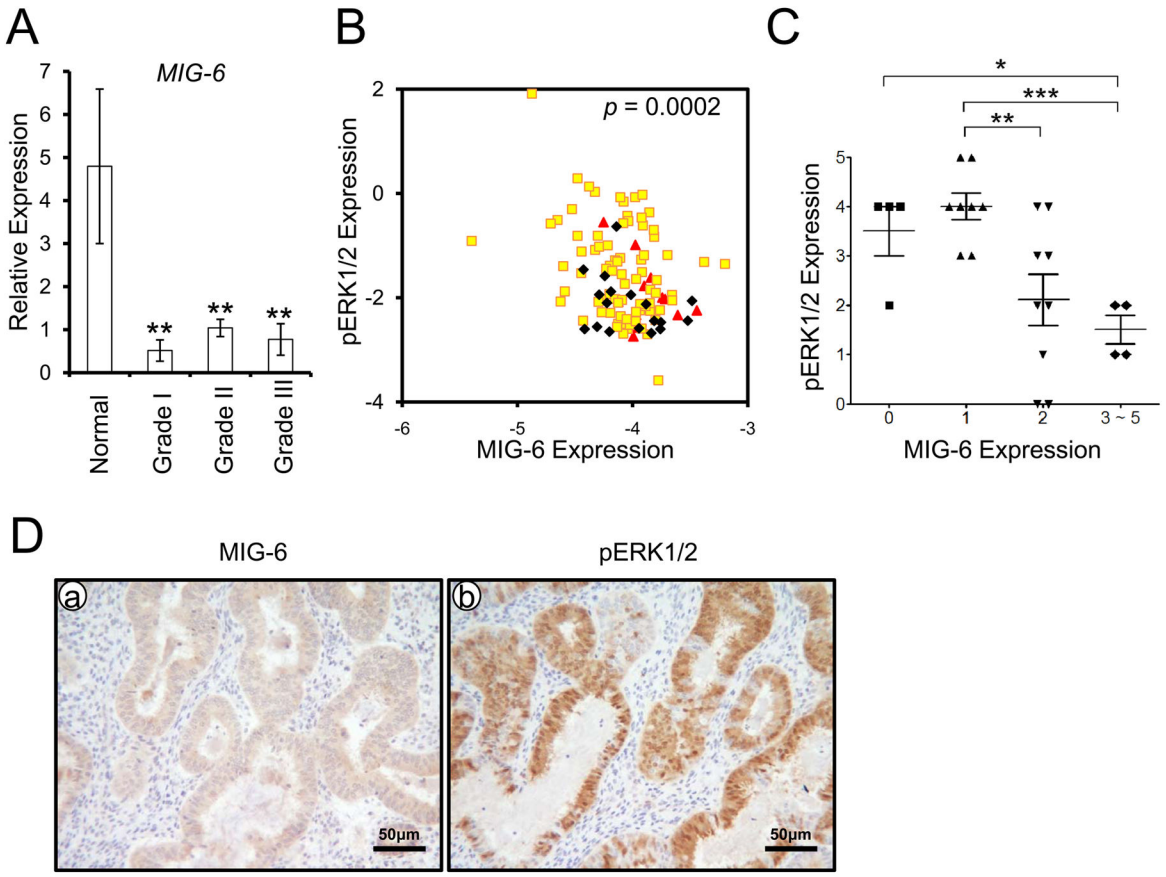

Figure 7.

The inverse correlation between MIG-6 and phospho-ERK1/2. (A) The expression of *MIG-6* is significantly decreased in endometrial cancer (n=5 of normal, n= 7 of grade I, n=10 of grade II and n=8 of grade III). The results represent the mean ± SEM. ** $p<0.01$. (B) The inverse correlation of MIG-6 and pERK1/2 in human endometrial cancer (red color for grade I (n=12), yellow color for grade II (n=79) and black color grade III (n=18) by Reverse Phase Protein Array. The correlation coefficient is −0.3467. (C) MIG-6 and phospho-ERK1/2 was scored by measuring expression intensity of endometrial epithelial cells from human endometrial cancer (n= 23 of grade I, n=10 of grade II and n=10 of grade III). The results represent the mean ± SEM. *** $p<0.001$, ** $p<0.01$, * $p<0.05$. (D) Photomicrographs represent inverse immunostaining for MIG-6 and phospho-ERK1/2 in human endometrial cancer.